Journal of Solid State Chemistry **147,** 320–327 (1999)
Article ID jssc.1999.8289, available online at http://www.idealibrary.com on IDEAL®

Electronic Instabilities and Localization Effects in the Quasi-Two-Dimensional Monophosphate Tungsten Bronzes $(PO_2)_4(WO_3)_{2m}$ and $K_xP_4W_8O_{32}$

J. Dumas,* U. Beierlein,* S. Drouard,* C. Hess,* D. Groult,† Ph. Labbé,† P. Roussel,† G. Bonfait,‡,§ E. Gomez Marin,‡ and C. Schlenker*

*Laboratoire d'Etudes des Propriétés Electroniques des Solides, CNRS, B.P. 166, 38042 Grenoble Cedex 9, France; †Laboratoire CRISMAT, CNRS UMR 6508, ISMRA, Université de Caen, 6 Bd Maréchal Juin, 14050 Caen Cedex, France; ‡Departamento de Quimica, ITN, P-2686 Sacavem Codex, Portugal; and §Physics Department, FCT, UNL, 2825 Monte de Caparica, Portugal

Received November 17, 1998; in revised form March 15, 1999; accepted March 23, 1999

The monophosphate tungsten bronzes $(PO_2)_4(WO_3)_{2m}$ with pentagonal tunnels are quasi-two-dimensional conductors that show charge density wave type electronic instabilities. These series of compounds provide a model system where the low-dimensional character and the average electron concentration are functions of the *m* parameter. The low *m* compounds ($m = 4, 6$) show conventional charge density wave instabilities. The $m = 5$ compound exists with two different crystal structures and shows instabilities with slightly different properties. We report measurements of transport properties for the compounds $m = 5, 7, 8, 9$. We show that, for $m > 7$, these compounds exhibit an upturn of resistivity and field dependence of the magnetoresistance characteristic of quantum interference effects. We also report transport properties of the compounds $K_xP_4W_8O_{32}$ with pseudo-hexagonal tunnels that show electronic instabilities with critical temperatures depending on *x*. © 1999 Academic Press

Key Words: **charge density wave; magnetotransport; localization; low dimensional.**

INTRODUCTION

Low-dimensional metallic oxides exhibit two types of electronic instabilities: Peierls type transition toward a charge density wave (CDW) state or superconducting instability. The existence of Peierls transitions is associated to Fermi surfaces (FS) showing nesting properties in the normal state. These instabilities give rise to gap openings on the FS and to either metal–semiconductor transitions or metal–metal transitions if electron and hole pockets are left on the Fermi surface. This is the case of the quasi-2D monophosphate tungsten bronzes with the general formula $(PO_2)_4(WO_3)_{2m}$, where m can be varied from 4 to 14 (1–5).

These series of compounds have been synthesized and their crystal structures studied more than a decade ago (6). Their lattice is orthorhombic or monoclinic (pseudo-orthorhombic) with pentagonal tunnels. It is built with ReO_3-type infinite layers of WO_6 octahedra parallel to the (a, b) plane, separated by PO_4 tetrahedra. Since the 5*d* conduction electrons are located in the perovskite $[WO_3]$-type slabs, the electronic properties are quasi-2D and the Fermi surface in the normal state is quasi-cylindrical. The thickness of the perovskite $[WO_3]$-type slabs, and therefore the c parameter, is increasing with m, while a and b weakly depend on it. A typical example of the crystal structure is given in Fig. 1a for the $m = 6$ compound.

The number of 5*d* electrons per primitive cell is always 4 regardless the value of m, while the average number of conduction electrons per W atom is $2/m$. The carrier density is therefore decreasing with m. This may lead to a weaker screening and to an increase of electron–electron interactions. These compounds show high Peierls temperatures, above room temperature for large values of m (4). A typical example of charge density wave instabilities revealed by resistivity measurements is shown in Fig. 1b for an $m = 6$ compound. Two anomalies are observed at $T_{p1} = 120$ K and $T_{p2} = 62$ K (4). X-ray diffuse scattering (XRDS) studies have shown that they correspond to incommensurate CDW with wave vector components in the (a, b) plane $q_1 = (0.385, 0)$ and $q_2 = (0.310, 0.295)$. A third instability has also been detected at $T_{p3} = 30$ K by X-ray with a wave vector $q_3 = (0.29, 0.11)$ (4, 9). One should note in Fig. 1b that a giant positive magnetoresistance is found at low temperatures when the magnetic field is perpendicular to the (a, b) plane. The compound $m = 4$ shows two Peierls transitions at $T_{p1} = 80$ K and $T_{p2} = 52$ K revealed by resistivity and XRDS measurements. XRDS studies show that they correspond to an incommensurate CDW with wave vector components in the (a, b) plane $q_1 = (0.330, 0.295)$ and $q_2 = (0.340, 0)$ (4, 9).

0022-4596/99 $30.00

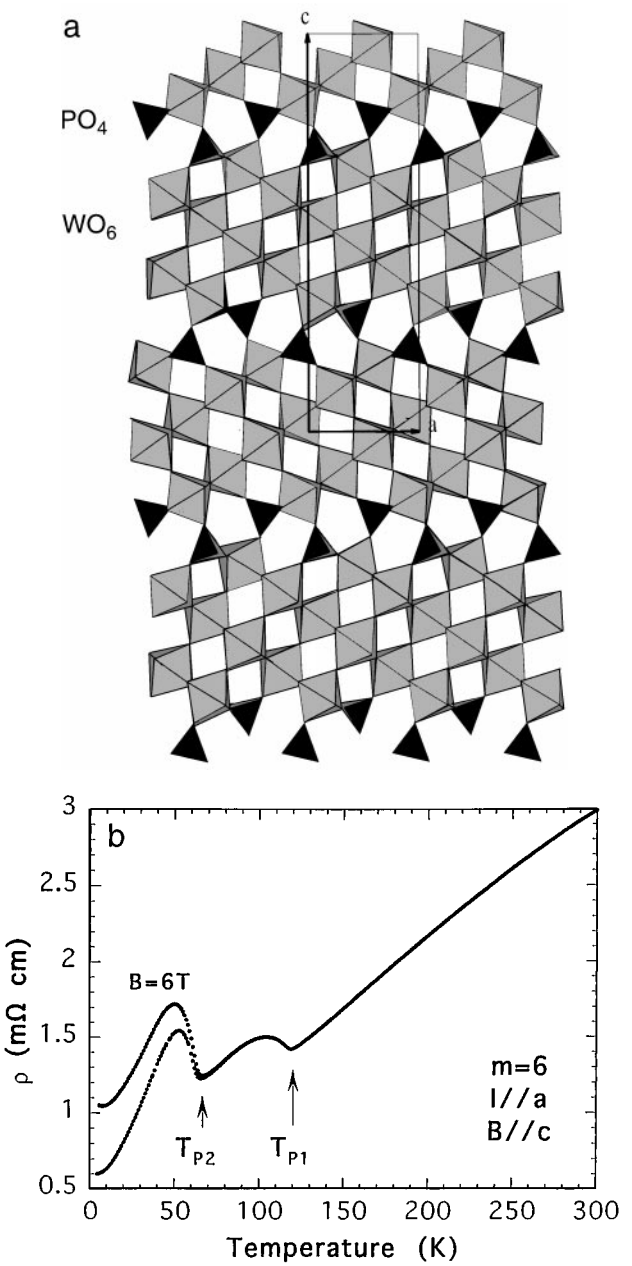

FIG. 1. (a) Crystal structure of $P_4W_{12}O_{44}$ ($m = 6$) showing the WO_6 octahedra and PO_4 tetrahedra (from Ref. 6). (b) Resistivity of an $m = 6$ sample as a function of temperature for magnetic field $B = 0$ and $B = 6$ T.

Band structure calculations using a tight binding extended Hückel method in a 2D approximation have been performed (7). Three bands cross the Fermi level. Nesting properties appear on the resulting Fermi surface obtained from the superposition of the three corresponding sheets. This is the so-called hidden nesting or hidden one dimensionality, due to the presence of infinite chains of WO_6 octahedra along the a, $(a + b)$, and $(a - b)$ axes. In this approximation, the Fermi surface can be viewed as the superposition of three quasi-1D Fermi surfaces.

Both the low-dimensional character and the average conduction electron density can be varied with the m parameter. One can also vary the conduction band filling by inserting an alkaline element in the structure. This is the case in $K_xP_4W_8O_{32}$ with pseudo-hexagonal tunnels where the average number of conduction electron per W site is $(4 + x)/8$ (8).

This article focuses on the series of monophosphate tungsten bronzes $(PO_2)_4(WO_3)_{2m}$ with $m = 5$, 7, 8, 9 and on the compounds $K_xP_4W_8O_{32}$ for which a $T_c(x)$ phase diagram is given.

EXPERIMENTAL

Single crystals used in these studies have been grown by chemical vapor transport technique (10, 11). The crystals are platelets parallel to the (a, b) conducting plane and have typical size ($2 \times 0.5 \times 0.05$ mm^3). In the case of $K_xP_4W_8O_{32}$, crystals as large as $6 \times 2 \times 0.4$ mm^3 have been obtained by this method (12). To obtain low contact resistance, the samples were washed in acetone and then in a 20% HF bath for 1 h; rapidly after this washing, silver pads of 500 Å were evaporated: contact resistance typically less than 10 Ω was obtained. Due to the anisotropic transport properties of these compounds, special care was taken to optimize the homogeneity of the current lines: the silver pads were evaporated to cover also the edge of the samples. With this method, unnested voltage (13) less than 10% of the measured voltage was easily obtained. This indicates that good ohmic contacts were obtained.

RESULTS

1. *Transport Properties and Instabilities in the Two $m = 5$ Structural Varieties*

The $m = 5$ compound is different from the other members of the series. Contrary to the others, it exists with two different structures leading to different transport properties. In the first type, the crystal structure is built with alternate layers of WO_6 octahedra of different thickness: the structure can be viewed as a regular intergrowth of $m = 4$ and $m = 6$ compound (6). In this case, an anomaly of the resistivity vs temperature at $T \sim 160$ K and a weaker one at ~ 30 K have been found, as illustrated in Fig. 2a. The anomaly at ~ 160 K is observed in the thermoelectric power S vs temperature, as shown in Fig. 2b. S is always negative. The change of the slope dS/dT below ~ 160 K may indicate that electron pockets become predominant in this temperature range and that hole pockets become again dominant at lower temperatures. The high temperature anomaly should be associated with a Peierls instability since a structural transition is observed at the same temperature (9).

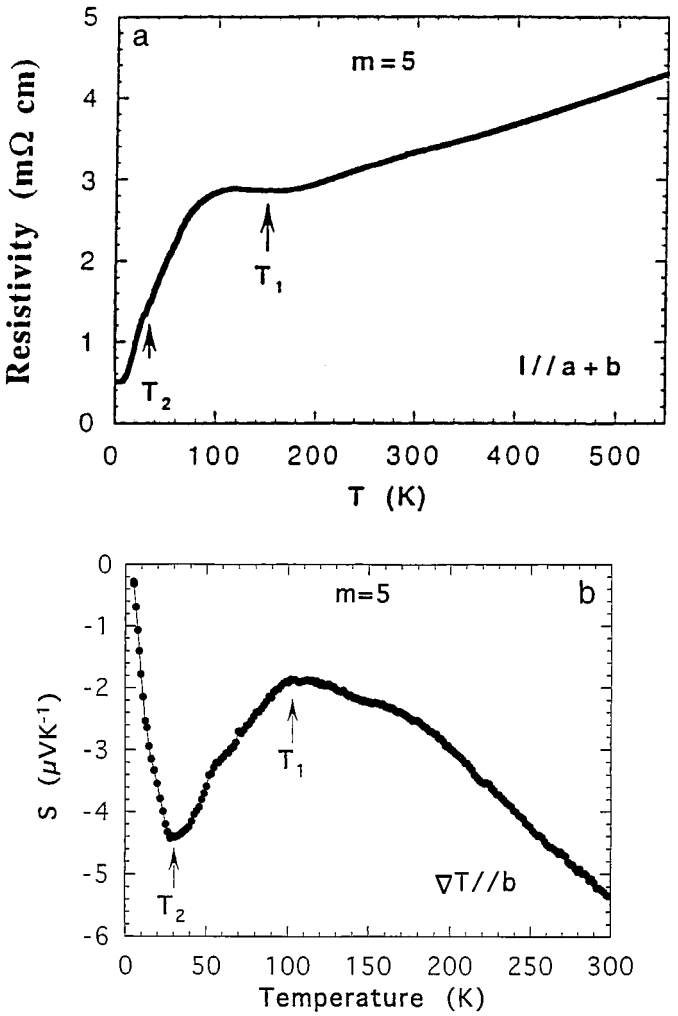

FIG. 2. (a) Resistivity of an $m = 5$ sample with an alternate 4/6/4/6 structure as a function of temperature. (b) Thermoelectric power of an $m = 5$ sample with an alternate 4/6/4/6 structure as a function of temperature.

In the second type, the crystal structure is made of a regular stacking of WO_6 octahedra slabs, all with the same thickness corresponding to the succession 5/5/5. Only one anomaly in the resistance vs temperature curve is detected at $T \sim 60$ K, as shown in Fig. 3a. This anomaly is also marked by a rather abrupt change in the slope dS/dT in the thermoelectric power vs temperature curve, as indicated in Fig. 3b (14).

Two structural instabilities have been found by XRDS studies, one at ~ 60 K the other at ~ 80 K, with weak satellite intensities (15). Our transport data support the presence of a partial Peierls gap opening onset at 60 K which would affect only a small portion of the Fermi surface.

2. *Charge Density Wave Instabilities and Quantum Interference Effects in the m = 7, 8, 9 Compounds*

The resistivity of the $m = 7$ compound has been measured down to 0.3 K. Below room temperature, on decreasing the temperature, the resistivity increases up to 170 K where an abrupt change occurs, associated to the first Peierls transition at $T_{p1} = 188$ K (Fig. 4a). Below this temperature, the resistivity still increases, reaches a rather sharp maximum ($\sim$165 K), and decreases down to a broad minimum (3). The $\rho(T)$ curve shows thermal hysteresis between ~ 100 K and T_{p1}. At $T = 0.3$ K, this compound enters a superconducting phase described elesewhere (16). To our knowledge, this compound is the first superconducting quasi-two-dimensional transition metal oxide bronze. On Fig. 4a is also shown the resistivity curve obtained with a magnetic field of 16 T applied parallel to the c axis. The resistivity behavior is not strongly modified by the magnetic field, the main difference being a more pronounced

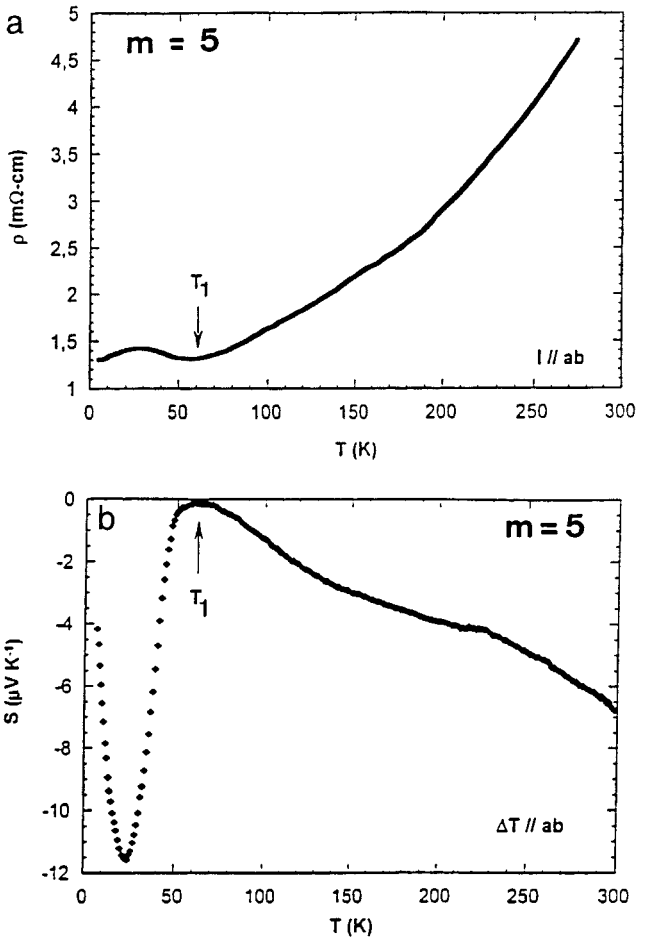

FIG. 3. (a) Resistivity of an $m = 5$ sample with a regular 5/5/5 structure as a function of temperature. (b) Thermoelectric power of an $m = 5$ sample with a regular 5/5/5 structure as a function of temperature.

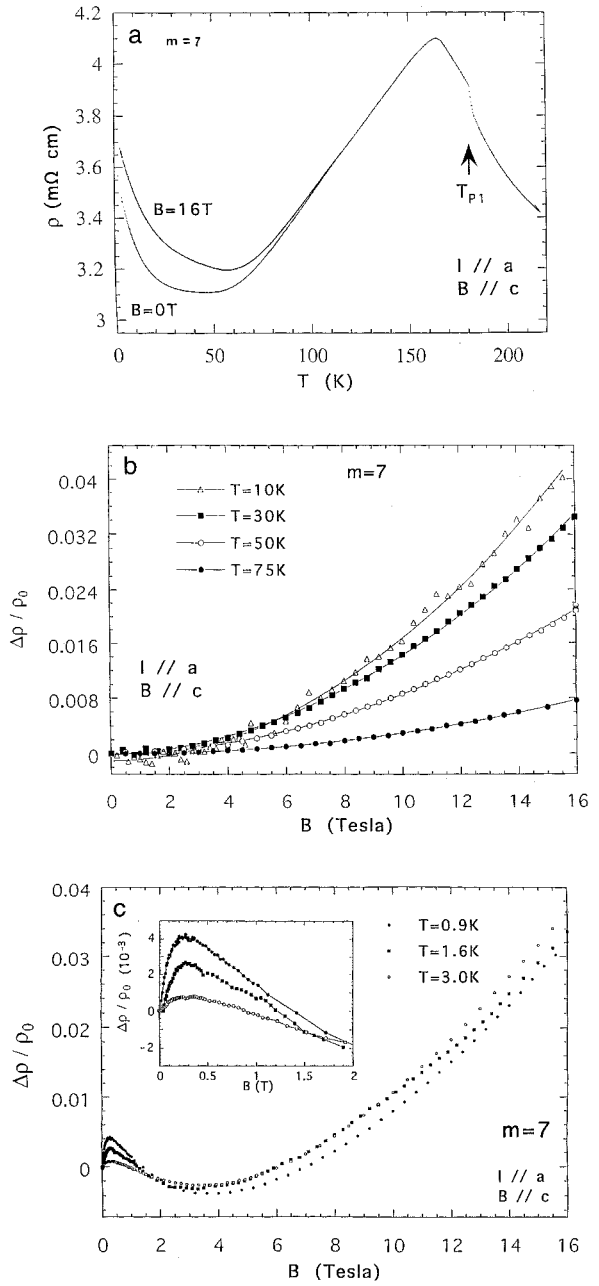

FIG. 4. (a) Resistivity and magnetoresistivity of an $m = 7$ sample. (b) Magnetoresistance of an $m = 7$ sample as a function of magnetic field at indicated temperatures. (c) Magnetoresistance of an $m = 7$ sample as a function of magnetic field at low temperatures ($T < 3$ K); current along the crystallographic a direction and magnetic field along c. The insert shows the low-field part of the magnetoresistance.

resistivity minimum shifted to a higher temperature (~ 60 K). A second transition at $T_{p2} = 60$ K has been detected by X-ray studies only (9). Both transitions are associated with the existence of several harmonics of the incommensurate CDW satellite wave vectors.

For $T > 10$ K, the magnetoresistance (MR) increases quadratically with magnetic field (Fig. 4b). At lower temperatures (Fig. 4c), the MR is more complex: it first increases up to $B \sim 0.3$ T and then decreases and passes through a large minimum before it reaches a quadratic regime similar to that obtained at high temperature. This low-field behavior is reminiscent of what occurs in some disordered systems (17).

In the $m = 8$ member, two incommensurate CDW modulations are detected by XRDS studies but no long-range order is achieved by cooling down to the lowest measurement temperature of ~ 35 K (9). Only a short-range order can be observed. The resistivity of the $m = 8$ compound was measured between 0.3 and 600 K (Fig. 5a). At high temperature ($T > 300$ K), the resistivity is metallic type ($d\rho/dT > 0$). A broad minimum occurs just below room temperature and for some samples a very weak change in slope can be detected at the Peierls transitions ($T_{p1} \sim 220$ K, $T_{p2} \sim 200$ K). The increase of the resistivity on lowering temperature becomes faster below 50 K.

The MR of the $m = 8$ compound is positive on the whole explored range of temperature and magnetic field. However, as in the $m = 7$ compound, two temperature ranges for the MR must be considered. Below 10 K (Fig. 5b), the MR varies rapidly for fields up to 0.5 T and slows down at higher field. For $T > 10$ K, a quadratic regime is reached similar to that obtained in the $m = 7$ compound (Fig. 5c).

In the $m = 9$ member, two commensurate CDW modulations toward a long-range order occur. The existence of higher order harmonics of the CDW satellites show that the instabilities are not conventional Peierls transitions (9). The resistivity of the $m = 9$ compound was measured between 0.3 and 580 K (Fig. 6a). The resistivity coefficient $d\rho/dT$ is always negative down to ~ 200 K and the Peierls transitions ($T_{p1} = 565$ K, $T_{p2} = 330$ K), as obtained by XRDS studies, are not clearly identified on the $\rho(T)$ curve. Below 50 K, similar to the $m = 7$ and $m = 8$ compounds, the resistivity increases with decreasing temperature. No sign of superconductivity was detected down to 0.3 K.

The MR behaves similarly to that of the $m = 7$ compound: at low T, the MR increases linearly with magnetic field (Fig. 6b) up to 7 T and slowly decreases at higher fields. The field corresponding to the maximum of the MR (~ 7 T) is approximately temperature independent and is found to be much higher than that found for the $m = 7$ compound (0.3 T). At higher temperature (Fig. 6c), the B^2 regime is recovered.

3. *Instabilities in $K_xP_4W_8O_{32}$*

The structure of $K_xP_4W_8O_{32}$ is similar to that of $(PO_2)_4(WO_3)_{2m}$ (12). However, the unit cell is now monoclinic due to a different arrangement of two successive WO_3-type slabs and the tunnels that are primarily pseudo-

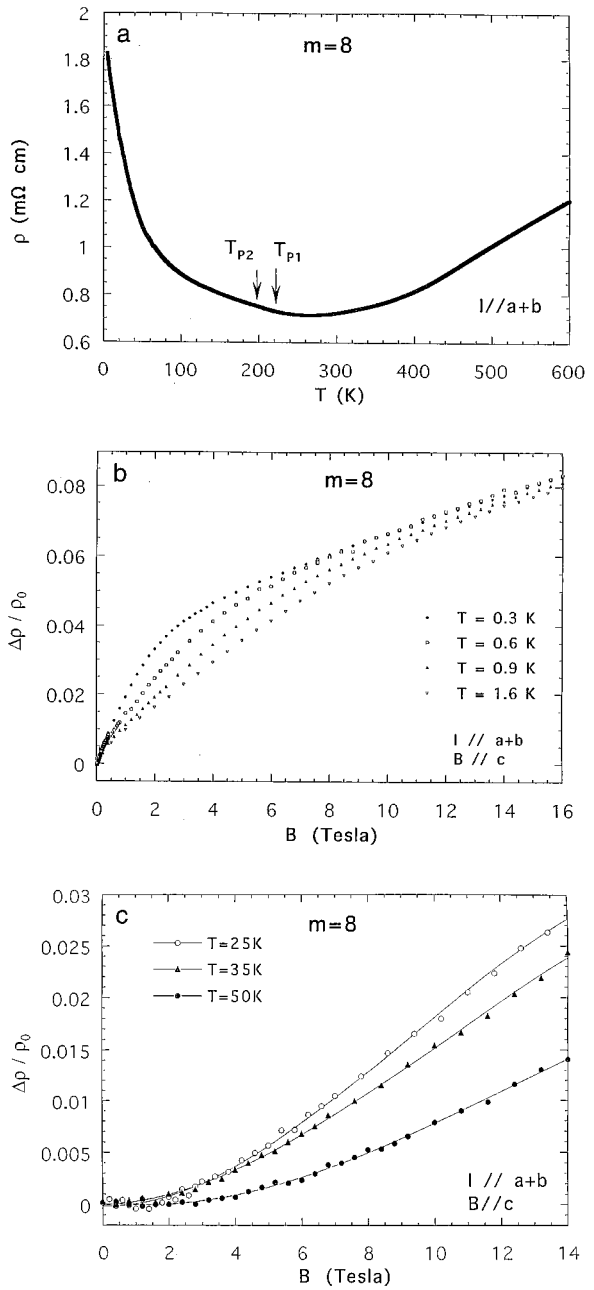

FIG. 5. (a) Resistivity vs temperature for an $m = 8$ sample; current along $(a + b)$ axis. T_{p1} and T_{p2} are the Peierls transition temperatures obtained by XRDS measurements (9). (b) Magnetoresistance vs magnetic field at $T < 1.6$ K for an $m = 8$ sample; $B//c$. (c) Magnetoresistance vs magnetic field at indicated temperatures; $B//c$; $I//(a + b)$.

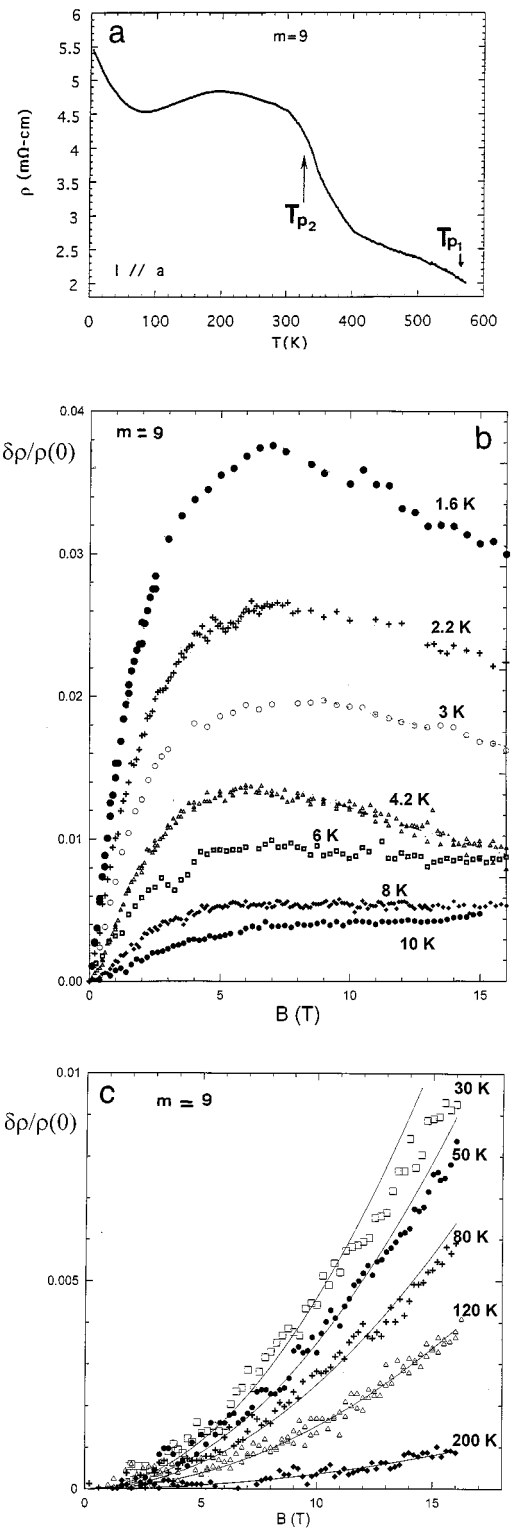

FIG. 6. (a) Resistivity as a function of temperature for an $m = 9$ sample; current along the a direction. T_{p1} and T_{p2} are the Peierls transition temperatures obtained by XRDS measurements (9). (b) Magnetoresistance as a function of magnetic field for an $m = 9$ sample at $T < 10$ K. (c) Magnetoresistance as a function of magnetic field for an $m = 9$ sample at $T > 30$ K. Solid lines are fits according to a quadratic law.

pentagonal become pseudo-hexagonal. In these tunnels there are four crystallographic sites that can be statistically occupied by the K atoms whose content x can vary from $x = 0.75$ to $x = 2$. The crystal structure is illustrated in Figs. 7a and 7b. Changing x leads to a change of the conduction band filling. Band structure calculations

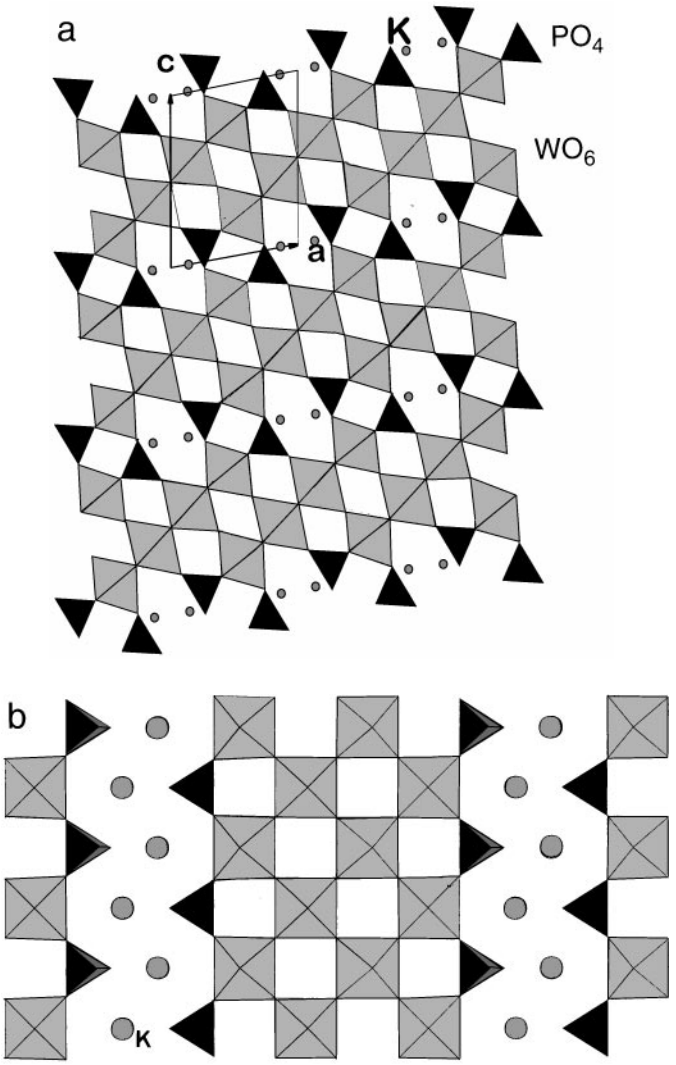

FIG. 7. (a) Projection along b of the crystal structure of $K_xP_4W_8O_{32}$. (b) Section of a slab of WO_3-type normal to an axis of the WO_6 octahedron.

performed with $x = 0.8$ show Fermi surface nesting properties similar to those of $(PO_2)_4(WO_3)_{2m}$ (18).

Figures 8a and 8b show the resistivity versus temperature curves for $0.86 < x < 1.94$. ρ is characteristic of a metal showing an anomaly at a temperature $T_c(x)$ marked by a minimum followed by a small hump and a decrease of ρ at lower temperatures. In contrast to the $m > 7$ undoped compound, no upturn of resistivity at low temperatures is observed. The curve $T_c(x)$ first increases with x from $T_c = 135$ K ($x = 0.86$) to a maximum of $T_c = 165$ K for $x = 1.30$. T_c then decreases reaching 80 K for $x = 1.94$ (Fig. 9). A large positive magnetoresistance is observed at low temperatures. It increases quadratically with the magnetic field. Its anisotropy is consistent with a quasi-cylindrical Fermi surface (19). XRDS studies (19) show that the wave vector of the modulation does not change with the band filling related to x. The satellite reflexions appear at a commensurate value $q = 0.50a^*$.

DISCUSSION

Let us now summarize first the main experimental results on the $m = 7, 8, 9$ compounds and compare them to those obtained on the low m compounds ($m = 4, 5, 6$). All three compounds with $m = 7, 8, 9$ show an increase in resistivity at low temperatures upon cooling while for low m compounds resistivity saturates. At low temperatures ($T < 50$ K), the resistivity coefficient $d\rho/dT$ of the "high-m compounds" is always negative in contrast to "the low-m compounds" family, in which the resistivity behavior at low T is similar to that of a metal with a residual resistivity less than 1 mΩ.cm. For the high-m compounds, the resistivity at low temperatures is larger than 1 mΩ.cm. The MR at low T does not show any Shubnikov–de Haas oscillations as observed in the $m = 4$, 6 and $m = 5$ with alternate 4/6/4/6

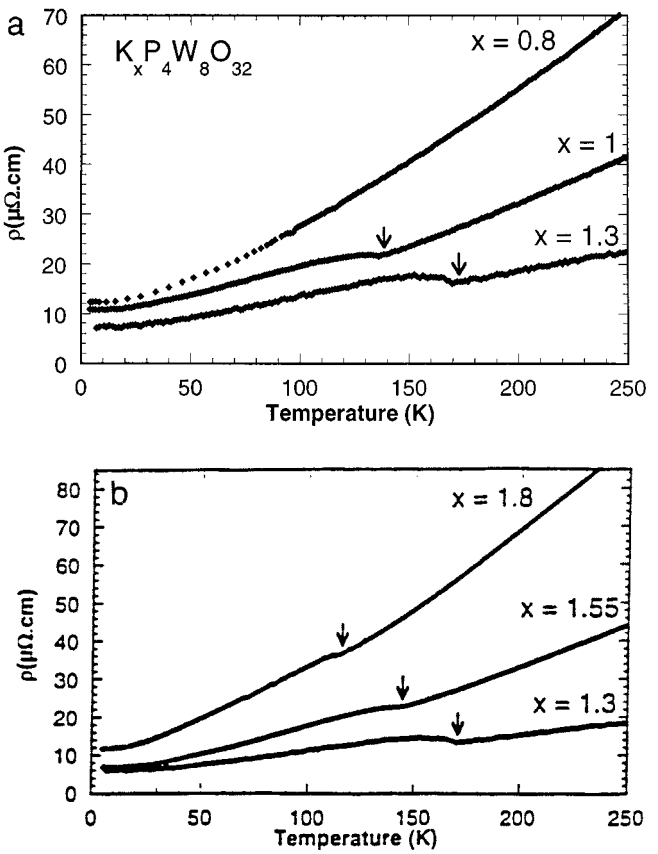

FIG. 8. (a) Resistivity vs temperature of $K_xP_4W_8O_{32}$ samples for $0.8 < x < 1.30$. (b) Resistivity vs temperature of $K_xP_4W_8O_{32}$ samples for $1.30 < x < 1.8$.

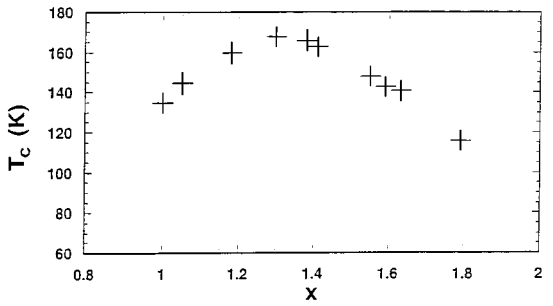

FIG. 9. Transition temperature T_c as a function of the K concentration x for $K_xP_4W_8O_{32}$.

structure compounds (20). The MR is comparatively small: for instance, at 4.2 K and 6 T, $\Delta\rho/\rho$ is always less than 3%, whereas for the low-m family, under the same conditions, $\Delta\rho/\rho$ is of order of 100%. The basic interpretation of these transport measurements at low T needs a model more elaborated than that of the nearly free electrons used for the low-m compounds. These results are discussed in the context of quantum interference effects (QIE), which are due to an elastic mean free path that is short compared to the inelastic one.

The Peierls instability in the $m = 7$ compound appears as an anomaly on the resistivity vs temperature curve. At temperatures above T_{p1}, the increase in ρ on lowering the temperature could be due to the existence of a pseudogap. This has been suggested earlier with respect to pretransitional streaks on the X-ray patterns (21). The observed increase in ρ below T_{p1} is a general feature of Peierls transitions and is attributed to a loss of carriers as the Peierls gap opens. At lower temperatures, the CDW state of $m = 7$ is characterized by a metallic behavior of the resistivity associated with the remaining parts of the Fermi surface. The strong thermal hysteresis, which has also been observed on the intensity of CDW satellite reflections, is not understood at the moment. It could be due to metastable configurations of CDW. A second CDW transition has been observed by X-ray studies at $T_{p2} = 60$ K. It does not appear as a distinct anomaly on the resistivity curve as for T_{p1}. One may note that both charge density wave anomalies in this compound are associated with nonsinusoidal modulations of the satellite wave vectors and therefore unconventional CDW states.

The $m = 8$ compound shows two successive Peierls instabilities. Unlike all other compounds of the series, the associated CDW–wave vectors of both transitions do not condense into distinct satellite spots even at the lowest temperatures as revealed by XRDS studies (9). This implies that the CDWs are correlated over a finite distance only. The minimum at ~ 260 K and the increase in ρ at lower temperatures might be due to the gradual opening of Peierls gaps at T_{p1} and T_{p2}. However, one also has to consider the possibility of an intrinsic disorder caused by the uncorrelated CDWs that could decrease the conductivity. The minimum of ρ at 260 K and the very weak anomalies at T_{p1} and T_{p2} could be a hint to pseudogap regime above the Peierls transitions, similar to the one suggested for $m = 7$.

Resistivity vs temperature data on $m = 9$ do not reveal any anomaly at $T_{p1} = 565$ K. One should note that the slope $d\rho/dT$ is negative in the normal and CDW states in the $m = 9$ as well as in the $m = 7$ compound. The broad maximum of the resistivity could be due to the gradual opening of the Peierls gap, affecting the Fermi surface and the charge carriers.

As mentioned above, the localization properties found at low temperatures in the $m \geq 7$ compounds may be due to QIE. This is related to comparatively short elastic mean free paths in these materials. Two contributions to the QIE are usually considered: the so-called weak localization if electron–electron interactions can be neglected and the so-called electron–electron interaction in the other case.

In the weak localization regime, the properties depend on several types of scattering times, namely, an inelastic scattering time τ_{ie}, a spin-orbit scattering time τ_{so} and a magnetic scattering time τ_B. The magnetic scattering time depends on the magnetic field and is related to a diffusion constant D through $\tau_B = \hbar/4eD\mathrm{B}$. The diffusion constant D may be evaluated from the Einstein relation $D = 1/\rho n(\varepsilon_F)e^2$ where $n(\varepsilon_F)$ is the density of states at the Fermi level. For example, in the $m = 7$ compound, using the data of Ref. (22) for the linear contribution to the specific heat, γT, with $\gamma = \pi^2 k_B^2 n(\varepsilon_F)/3$, ($\gamma = 136$ mJ mole^{-1} K^{-2}) one estimates D to be at 1.6 K of the order of 5×10^{-2} cm^2 s^{-1}. This low diffusivity value is comparable to what is found in a number of transition metal oxides (such as the class of ABO_3 compounds) showing weak localization effects (23). A weak localization model is therefore appropriate.

The anomalous field dependence of the magnetoresistance of the $m = 7$ compound at low temperatures (Fig. 4c) can thus be discussed along these lines. One expects a change in sign of $\Delta\rho/\rho$ in some intermediate field range (24). This is not inconsistent with the data for $m = 7$ or $m = 9$ (Fig. 6b). These results are discussed in more detail in Ref. (25).

In the case of the $m = 8$ compound, the diffusion coefficient is evaluated at low temperature ($T \sim 1.6$ K) $D \sim 3.5 \times 10^{-1}$ cm^2 s^{-1}, using an experimental value for γ of 14 mJ mole^{-1} K^{-1} (25).

However, contrarily to the $m = 7$ compound, the magnetoresistance of the $m = 8$ compound is always positive and increases monotonically up to 16 T and down to 0.3 K. This behavior cannot be quantitatively explained by weak localization effects but rather by a consequence of electron–electron interactions.

The presence of quantum interference effects is due to an elastic mean free path that is short compared to the inelastic

one. This comparatively short elastic mean free path may have several origins, such as (i) the presence of impurities, (ii) the possibility of oxygen nonstoichiometry, and (iii) the possibility of stacking faults of WO_3 layers through more or less extended intergrowth defects as revealed by HREM studies (26). The probability of such defects which involve a local change of the m value increases as the thickness of the WO_3-type slabs increases.

One should note that in the $m = 8$ compound the CDW do not develop long-range order down to the lowest temperatures. These local uncorrelated Peierls lattice distortions may also have an effect on the transport properties and represent a possible source of intrinsic disorder besides the mechanisms mentioned above.

In $K_xP_4W_8O_{32}$, the coupled electronic and structural transition at T_c is not a simple Peierls transition. In the context of a Peierls-like transition, the absence of variation of the wave vector with x could be related to a change in the filling of a nonrigid three-band system. The value $x \sim 4/3$ for the maximum in the $T_c(x)$ curve corresponds on average to 2/3 electrons per W site. The T_c dependence on x suggests that the relative filling of the three bands crossing the Fermi level varies with x and is associated with strong electron–lattice coupling inducing a lock-in type transition. In the mean field approximation, the concentration $x \sim 4/3$ would correspond to a maximum of the density of states at the Fermi level, possibly related to two half-filled conduction bands and one empty conduction band.

CONCLUSION

In summary, the monophosphate tungsten bronzes provide a model system for quasi-two-dimensional conductors where the Peierls temperatures and the electrical resistivity can be varied as a function of the m parameter. Resistivity and magnetoresistance measurements have given information on the low-temperature CDW state of the $(PO_2)_4(WO_3)_{2m}$ phosphate tungsten bronzes for $m = 7$, 8, 9 and of $K_xP_4W_8O_{32}$. All compounds with $m > 7$ exhibit an upturn of resistivity at low temperatures. Quantum interference effects can explain the magnetoresistance data. In the $m = 7$ and $m = 9$ compounds, the weak localization mechanism is dominant while for $m = 8$ the main contribution seems to be the interaction between electrons. The $m = 7$ compound is a system that allows study of the interplay among charge density wave, superconductivity, and weak localization effects. In the case of $K_xP_4W_8O_{32}$, the origin of the coupled electronic and structural transition is not yet elucidated.

ACKNOWLEDGMENTS

This work was supported in part by the Human Capital and Mobility Programme of the European Union under Contract ERBCHRXCT940616.

REFERENCES

1. C. Schlenker (Ed.), "Low Dimensional Electronic Properties of Molybdenum Bronzes and Oxides." Kluwer Academic, Dordrecht/Norwell, MA, 1989.
2. M. Greenblatt (Ed.), *Int. J. Mod. Phys.* **B7,** 4045 (1993).
3. C. Schlenker, J. Dumas, M. Greenblatt, and S. van Smaalen (Eds.), "Physics and Chemistry of Low Dimensional Inorganic Conductors," NATO ASI Series B, Vol. 354. Plenum, New York, 1996.
4. C. Schlenker, C. Hess, C. Le Touze, and J. Dumas, *J. Phys. (France) I* **6,** 2061 (1996).
5. C. Hess, C. Schlenker, J. Dumas, M. Greenblatt, and Z. S. Teweldemedhin, *Phys. Rev. B* **54,** 4581 (1996).
6. J. P. Giroult, M. Goreau, Ph. Labbé, and B. Raveau, *Acta Crystallogr. Sect. B* **37,** 2139 (1981); A. Benmoussa, Ph. Labbé, D. Groult, and B. Raveau, *J. Solid State Chem.* **44,** 318 (1982); Ph. Labbé, M. Goreaud, and B. Raveau, *J. Solid State Chem.* **61,** 324 (1986); M. Borel, M. Goreaud, A. Grandin, Ph. Labbé, A. Leclaire, and B. Raveau, *Eur. J. Solid Inorg. Chem.* **28,** 93 (1991).
7. E. Canadell and M. Whangbo, *Phys. Rev. B* **43,** 1894 (1990); in Ref. 3, p. 271.
8. P. Roussel, D. Groult, C. Hess, Ph. Labbé, and C. Schlenker, *J. Phys. Condens. Matter* **9,** 708 (1997).
9. A. Ottolenghi and J. P. Pouget, *J. Phys. I* **6,** 1059 (1996).
10. P. Roussel, Ph. Labbé, D. Groult, B. Domengès, H. Leligny, and D. Grebille, *J. Solid State Chem.* **122,** 281 (1996).
11. Z. S. Teweldemedhin, K. V. Ramanujachary, and M. Greenblatt, *J. Solid State Chem.* **95,** 21 (1991).
12. J. P. Giroult, M. Goreaud, Ph. Labbé, and B. Raveau, *J. Solid State Chem.* **44,** 407 (1982).
13. D. E. Schafer, F. Wudl, G. A. Thomas, J. P. Ferraris, and D. O. Cowan, *Solid State Commun.* **14,** 347 (1974).
14. U. Beierlein, C. Schlenker, J. Dumas, D. Groult, Ph. Labbé, E. Balthes, and E. Steep, *in* "International Conference on Synthetic Metals, ICSM 98," Synthetic Metals, to be published.
15. P. Foury, P. Roussel, D. Groult, and J. P. Pouget, *in* "International Conference on Synthetic Metals, ICSM98," Synthetic Metals, to be published.
16. C. Hess, C. Schlenker, G. Bonfait, J. Marcus, T. Ohm, C. Paulsen, J. Dumas, J.-L. Tholence, M. Greenblatt, and M. Almeida, *Physica C* **282–287,** 955 (1997); C. Hess, C. Schlenker, G. Bonfait, T. Ohm, C. Paulsen, J. Dumas, Z. Teweldemedhin, M. Greenblatt, J. Marcus, and M. Almeida, *Solid State Commun.* **104,** 663 (1997).
17. G. Bergmann, *Phys. Rep.* **107,** 1 (1984).
18. E. Canadell and M. Whangbo, *Phys. Rev. B* **43,** 1894 (1991).
19. S. Drouard, P. Foury, P. Roussel, D. Groult, and J. Dumas, *in* "International Conference on Synthetic Metals, ICSM 98," Synthetic Metals, to be published.
20. C. Le Touze, G. Bonfait, C. Schlenker, J. Dumas, M. Almeida, M. Greenblatt, and Z. Teweldemedhin, *J. Phys. I* **5,** 437 (1995).
21. P. Foury and J. P. Pouget, *Int. J. Mod. Phys. B* **7,** 3973 (1993).
22. C. Le Touze, thesis, Université Joseph Fourier, Grenoble, 1996; J. Lehmann, C. Schlenker, C. Le Touze, A. Rötger, J. Dumas, J. Marcus, Z. Teweldemedhin, and M. Greenblatt, *J. Phys. (France) IV*, *Coll. C2* **3,** 243 (1993).
23. M. A. Dubson, D. F. Holcomb, *Phys. Rev. B* **32,** 1955 (1985); A. K. Raychaudchari, *Phys. Rev. B* **44,** 8572 (1991); A. K. Raychaudhuri, *Adv. Phys.* **44,** 21 (1995).
24. A. Kawabata, *Solid State Commun.* **34,** 431 (1980).
25. C. Hess, thesis, Université Joseph Fourier, Grenoble, 1997.
26. B. Domengès, private communication, 1996; B. Domengès, P. Roussel, Ph. Labbé, and D. Groult, *J. Solid State Chem.* **127,** 302 (1996).